Scarcity of fixed carbon transfer in a model microbial phototroph-heterotroph interaction

Short Title: Scarcity of microbial carbon transfer

Sunnyjoy Dupuis[1,2], Usha F. Lingappa[2], Xavier Mayali[3], Eve S. Sindermann[2], Jordan L. Chastain[2,4], Peter K. Weber[3], Rhona Stuart[3], Sabeeha S. Merchant[1,2,5,6]

[1]Department of Plant and Microbial Biology, University of California, Berkeley, CA 94720, USA

[2]California Institute for Quantitative Biosciences (QB3), University of California, Berkeley, CA 94720, USA

[3]Physical and Life Sciences Directorate, Lawrence Livermore National Laboratory, Livermore, CA 94550, USA

[4]College of Chemistry, University of California, Berkeley, CA 94720, USA

[5]Department of Molecular and Cell Biology, University of California, Berkeley, CA 94720, USA

[6]Division of Environmental Genomics and Systems Biology, Lawrence Berkeley National Laboratory, Berkeley, CA, USA

Correspondence: Sabeeha S. Merchant, sabeeha@berkeley.edu, +1 510 664-5154, 408B Stanley Hall, Berkeley, CA 94720-3220

Study Funding: This work was supported by The Gordon and Betty Moore Foundation Symbiosis in Aquatic Systems Initiative Investigator Award GBML9203, and the Lawrence Livermore National Laboratory µBiospheres Scientific Focus Area award SCW1039 from the DOE OBER Genomic Sciences Program. S.D. acknowledges support from NIH T32 Genetic Dissection of Cells and Organisms training grant 1T32GM132022-01.

ABSTRACT

While the green alga *Chlamydomonas reinhardtii* has long served as a reference organism, few studies have interrogated its role as a primary producer in microbial interactions. Here, we quantitatively investigated *C. reinhardtii's* capacity to support a heterotrophic microbe using the established coculture system with *Mesorhizobium japonicum*, a vitamin B_{12}-producing α-proteobacterium. Using stable isotope probing and nanoscale secondary ion mass spectrometry (nanoSIMS), we tracked the flow of photosynthetic fixed carbon and consequent bacterial biomass synthesis under continuous and diel light with single-cell resolution. We found that more ^{13}C fixed by the alga was taken up by bacterial cells under continuous light, invalidating the hypothesis that the alga's fermentative degradation of starch reserves during the night would boost *M. japonicum* heterotrophy. $^{15}NH_4$ assimilation rates and changes in cell size revealed that the carbon transferred was insufficient for balanced growth of *M. japonicum* cells, which instead underwent reductive division. However, despite this sign of starvation, *M. japonicum* still supported a B_{12}-dependent *C. reinhardtii* mutant. Finally, we showed that bacterial proliferation could be supported solely by the algal lysis that occurred in coculture, highlighting the role of necromass in carbon cycling. Collectively, these results reveal the scarcity of fixed carbon in this microbial trophic relationship, demonstrate B_{12} exchange even during bacterial starvation, and underscore the importance of quantitative approaches for assessing metabolic coupling in algal-bacterial interactions.

KEY WORDS

rhizobia; chlorophyte; photoautotroph; diurnal; cobalamin; co-cultivation; symbiosis; SIP

INTRODUCTION

Photosynthetic microbes are responsible for a large fraction of the primary productivity on our planet [1]. These organisms supply the microbial world with raw materials for life, thereby shaping communities and driving carbon cycling [2, 3]. Through exudation, lysis, and predation, photosynthetic microbes provide a variety of reduced carbon substrates with various diffusion rates and accessibility to heterotrophic bacteria. The primary consumers recycle carbon back to inorganic forms, closing the "microbial loop" that constitutes a major component of biogeochemical carbon cycling [2, 4, 5]. Heterotrophic bacteria can also influence algal productivity, for example, by changing the availability of critical micronutrients for algal growth and metabolism [6–8].

The green alga *Chlamydomonas reinhardtii* has served as a reference organism for discoveries in photosynthesis, cilia-based motility, and the eukaryotic cell cycle [9]. Extensive work on axenic (bacteria-free) cultures has provided detailed knowledge of the pathways and regulons for photosynthesis and primary metabolism. This chlorophyte has a flexible metabolic repertoire, with the capacity to grow by photoautotrophy alone or by acetate assimilation. Under diel cycles, *C. reinhardtii*'s metabolism is shaped by programmed waves of gene expression that accommodate rhythmic changes in light and oxygen availability that occur in natural environments [10, 11]. While extensive knowledge of its metabolism makes *C. reinhardtii* an attractive model organism to study microbial trophic interactions, relatively little is known about how *C. reinhardtii* contributes to its environment and influences its neighbors in the microbial world.

In its natural soil context, *C. reinhardtii* is surrounded by other microbes that exchange nutrients, compete for resources, and communicate with one another. *C. reinhardtii* can enrich for particular heterotrophic bacteria from bulk soil, demonstrating that the alga's growth can influence

67 the metabolisms and behaviors of various bacteria [12, 13]. Studies of *Chlamydomonas*-bacteria
68 interactions have primarily focused on impacts to the alga's behavior, in part due to technical
69 challenges in probing bacterial physiology in mixed cultures. Bacteria are known to supply
70 vitamins and fixed nitrogen, facilitate iron assimilation, and impart thermal tolerance to algal
71 cultures [6, 7, 14–20]. Coculture of *C. reinhardtii* with various heterotrophic bacteria (e.g.
72 *Bradyrhizobium japonicum*, *Pseudomonas* sp.) has been shown to stimulate algal H_2 production,
73 starch accumulation, and viability under sulfur deprivation by consuming O_2 and alleviating
74 accumulation of fermentation byproducts from the medium [21]. Bacterial secondary metabolites
75 can also influence *C. reinhardtii*'s cell cycle and aggregation [22, 23]. In addition, symbioses
76 between *C. reinhardtii* and vitamin B_{12}-producing rhizobia like *Mesorhizobium japonicum*
77 (previously referred to as *Mesorhizobium loti*), *Sinorhizobium meliloti*, and *Rhizobium*
78 *leguminosarum* have been used to study the evolution of vitamin dependency across the algal tree
79 of life [6, 15, 24–28]. *C. reinhardtii* does not require vitamin B_{12} for growth since it has retained
80 a functional cobalamin-independent isoform of methionine synthase, METE1. However, when
81 supplied vitamin B_{12}, transcription of *METE1* is repressed, and the vitamin is used as a cofactor
82 for the cobalamin-dependent isoform, METH1. When grown in the laboratory with a continuous
83 supply of the vitamin, *C. reinhardtii* acquired deleterious mutations in the repressed *METE1* gene
84 yielding B_{12}-requiring strains (*mete1*) in less than 500 generations of growth [25].

85 The interaction between the *C. reinhardtii mete1* mutant and *M. japonicum* has been
86 suggested to be facultatively mutualistic: the mutant alga receives the vitamin cofactor, and the
87 bacterium is believed to receive reduced carbon compounds that support heterotrophic growth.
88 The literature provides some clues of potential substrates that could be exchanged. *C. reinhardtii*
89 secretes small amounts of glycerol when grown in nitrogen deficient minimal medium in

90 continuous light, supporting some growth of cocultured *Methylobacterium* spp [29]. In dark and
91 anoxic conditions, *C. reinhardtii* produces formate, acetate, ethanol, and minor products lactate,
92 malate, and succinate, which could also be used by co-cultivated heterotrophs [30–35]. Rhizobia
93 are known to metabolize C4 dicarboxylic acids like succinate, malate, and fumarate, which are the
94 primary carbon sources in the root nodules of legumes where the bacterium persists in the bacteroid
95 form [36–39]. They can also utilize other organic acids present in plant root exudates [40], as well
96 as glycerol and sucrose. However, the mechanism and magnitude of the flux of carbon transfer
97 from *C. reinhardtii* to *M. japonicum* remains unclear.

98 Here, we quantified the transfer of fixed carbon from wild-type *C. reinhardtii* to *M.*
99 *japonicum* using stable isotope probing and nanoscale secondary ion mass spectrometry
100 (nanoSIMS). We found that a small but significant amount of photosynthetically fixed carbon was
101 taken up by the bacterial population, but that *M. japonicum* growth was severely limited, resulting
102 in reductive bacterial division. Thus, *C. reinhardtii* primary productivity yields a low carrying
103 capacity for this bacterium. Nonetheless, *M. japonicum* provided adequate B_{12} to enable growth of
104 the *C. reinhardtii mete1* strain even when the bacterium itself exhibited signs of starvation. These
105 results highlight that in natural contexts, bacterial populations may not proliferate to the cell
106 densities possible in the gourmand rich media often used in the laboratory, but they can still greatly
107 influence the metabolism and evolution of their neighbors in the microbial world.

108 **MATERIALS AND METHODS**

109 **Strains and culture conditions**

110 Three strains of *C. reinhardtii* were used in this study. The *mete1* strain generated through
111 experimental evolution on 1000 ng/l vitamin B_{12} [25] and its parental wild-type strain were
112 provided by Alison G. Smith (University of Cambridge, UK). For experiments testing the impact

113 of diel light, we used the cell-wall reduced strain CC-5390 [10]. This strain is amenable to
114 synchronization under diel cycles, providing a system with exceptional signal-to-noise for
115 resolving diel patterns. While CC-5390 exhibits a reduced cell wall, we found no significant
116 difference in the amount of nonpurgeable organic carbon (NPOC) released into the spent medium
117 between this strain and the other wild-type strain used (SI Fig. 1). *M. japonicum* strain
118 MAFF303099 was also provided by Alison G. Smith.

119 All experiments were performed in amended HSM minimal medium [41] with a modified
120 trace element solution [42], 2 mM $MgSO_4.7H_2O$, 10 µg/l biotin, and 10 µM $CoCl_2$ unless otherwise
121 specified. Cultures were grown in either 250 ml Erlenmeyer flasks containing 100 ml medium and
122 bubbled with filter-sterilized air (provided by an aquarium pump), 6-well plates with 3 ml medium,
123 or 250 ml beakers with 50 ml medium. Algal cultures and cocultures were incubated at 28°C,
124 agitated at 110–130 rpm, and illuminated with 200 µmol photons/m^2/s cool white light (Sylvania
125 Dulux L55WFT55DL/841) continuously or under diel 12-h-light/12-h-dark cycles.

126 *C. reinhardtii* cells were precultivated in photoautotrophic conditions for at least 3 passages
127 prior to experiments. The *mete1* strain was precultivated with 200–250 ng/l vitamin B_{12}
128 (cyanocobalamin), collected by centrifugation at 1000 x*g*, then gently resuspended in fresh
129 medium without B_{12} before use as inoculum. For experiments comparing coculture in continuous
130 light versus diel light, *C. reinhardtii* CC-5390 cells were precultivated in flat-panel
131 photobioreactors (Photon System Instruments, Drásov, Czechia) as previously described under the
132 respective light regime to achieve adequate synchrony of the diel populations [10].

133 Bacterial cells were precultivated in 14 ml polystyrene round bottom tubes with 3 ml
134 amended HSM containing 0.2% sucrose, agitated at 200 rpm, and incubated at 28°C. When larger
135 volumes were required for inoculation, cells were precultivated instead in 250 ml Erlenmeyer

136 flasks containing 100 ml medium, continuously bubbled with air, and agitated at 110–130 rpm.
137 Bacterial cells were collected by centrifugation at 8000 x*g* and washed three times in 0.85% NaCl
138 to remove sucrose before use as inoculum. Optical density (OD) at 600 nm was used to estimate
139 the cell density of washed cell suspensions used for inoculation.

140 **Cell number, size, and cytotoxicity measurements**

141 *C. reinhardtii* cell density and size were determined using a hemocytometer and ImageJ or
142 a Beckman Coulter Multisizer 3 with a 50 µm orifice (Beckman Coulter, CA, USA). Bacterial cell
143 density was determined by counting colony forming units (CFU) in 10 µl spots of serial dilutions
144 on Typtone Yeast (TY) agar medium after 4 d of incubation at 30°C in the dark.

145 Algal cellular integrity was estimated using CellTox Green Cytotoxicity Assay (Promega,
146 WI, USA). *C. reinhardtii* sample densities were adjusted to $1x10^5$–$1x10^6$ cells/ml. Triplicate killed
147 control samples were prepared by heating cells at 90°C for 10 min. Fluorescence was measured in
148 a black-walled 96-well plate using a SpectraMax iD3 plate reader (Molecular Devices, CA, USA).
149 Background fluorescence of a medium blank was subtracted from all values, and results were
150 reported relative to killed control samples.

151 Samples for fluorescence microscopy were fixed overnight in 4% paraformaldehyde at 4°C
152 in the dark. Fixed samples were then collected by centrifugation at 10,000 x*g*, washed in phosphate
153 buffered saline (PBS) (pH 7), and stored in 1:1 ethanol:PBS at -20°C. For imaging, samples were
154 spotted on 0.22 µm GTTP type isopore polycarbonate filters and washed with sterile water to
155 remove residual salts. Prepared filters were mounted on slides with 5 µg/ml DAPI in Citifluor
156 antifade mounting medium buffered with PBS and imaged using a Zeiss Axioimager M2
157 microscope with a DAPI filter set (Ex 350/50, Em 460/50) at the UC Berkeley Biological Imaging
158 Facility. Bacterial cell lengths were measured using ImageJ.

159 **Total organic carbon measurements**

160 Total nonpurgeable organic carbon content (NPOC) of cells was determined using a TOC-
161 L Shimadzu Total Organic Carbon Analyzer (Shimadzu, Kyoto, Japan). 10–40 ml culture was
162 collected by centrifugation at 8000 x*g* for 2 min, and the supernatant was collected and then stored
163 at -20°C until analysis. Spent media were diluted 2-fold and HCl was added to 27 mM. All samples
164 were sparged to remove inorganic carbon. Some organic carbon may be purged from the sample
165 by this method, so we report "nonpurgeable" organic carbon.

166 **Stable isotope labelling and nanoSIMS**

167 $^{15}NH_4Cl$ (99% ^{15}N, Cambridge Isotope Laboratories, MA, USA) was provided directly in
168 the culture medium, replacing 50% of the NH_4Cl in HSM. 13 h after inoculation, $^{13}CO_2$ was
169 provided to cultures by bubbling air through a solution of $NaH^{13}CO_3$ (99% ^{13}C, Cambridge Isotope
170 Laboratories) and then into the cultures as previously described [43]. Killed controls were
171 generated by treating cells with 4% paraformaldehyde for 20 min in the dark. Coculture
172 experiments were otherwise conducted as described above.

173 For nanoSIMS analyses, samples were fixed and deposited on filters as described above
174 for fluorescence microscopy. Dry filter pieces were then mounted on 1 inch round stubs using
175 carbon tabs (Ted Pella, Inc., CA, USA) and gold coated. Data were collected on a NanoSIMS 50
176 (CAMECA, Gennevilliers, France) using a 1.5 pA Cs^+ primary ion beam at the Lawrence
177 Livermore National Laboratory. The secondary ion masses of $^{12}C_2^-$, $^{12}C^{13}C^-$, $^{12}C^{14}N^-$, $^{12}C^{15}N^-$, and
178 $^{32}S^-$ were collected. Raw nanoSIMS images were processed using L'image (L. Nittler, Carnegie
179 Institution of Washington, D.C., USA). Individual cell regions of interest (ROIs) were manually
180 circled using size and high $^{12}C^{14}N$ signal to identify bacterial cells and high $^{12}C^{13}C$ signal along
181 with the secondary electron image to identify algal cells. Isotope enrichment in atom percent

182 enrichment (APE) for $^{12}C^{13}C^{-}/^{12}C_2^{-}$ and $^{12}C^{15}N^{-}/^{12}C^{14}N^{-}$ were calculated using standard ratios of
183 0.02247 and 0.00367, respectively. Enrichment data are also presented as net assimilation (N_{net}
184 and C_{net}), the fraction of newly synthesized biomass relative to total biomass, as defined by Dekas
185 *et al.* 2019, calculated against an unlabeled biomass standard [44]. For ^{15}N, net assimilation was
186 calculated using the known isotopic composition of the initial source substrate added to the
187 medium. For ^{13}C, net bacterial assimilation was calculated using the average algal biomass
188 composition in each experiment as a rough estimation of the source substrate.

189 **Spent medium and cell lysate experiment**

190 Wild-type *C. reinhardtii* was grown for 48 h in continuous light until density reached 1–
191 $4x10^6$ cells/ml. Cells were collected by centrifugation in 500 ml polypropylene bottles for 4 min
192 at 11,900 x*g* and 4°C. The supernatant was passed through a 0.22 µM filter to generate sterile spent
193 medium. Cell pellets were resuspended in fresh medium and then sonicated using a Fisherbrand
194 Model 505 Sonic Dismembrator (Fisher Scientific, PA, USA) on ice for 45 min with alternating
195 10 s at 30% intensity, 15 s "off" steps. The supernatant of the resulting cell lysate was then passed
196 through a 0.22 µM filter to generate sterile soluble cell lysate. Spent medium, soluble cell lysate,
197 and parallel live *C. reinhardtii* cultures were then inoculated with *M. japonicum* as described
198 above, and growth was monitored over another 48 h.

199 **RESULTS**

200 ***M. japonicum* growth is severely limited in coculture with *C. reinhardtii*, especially under diel**
201 **light**

202 Previous work suggested that *C. reinhardtii* supports heterotrophic growth of the rhizobial
203 bacterium *M. japonicum* when cocultured in minimal medium given light and atmospheric CO_2
204 [25–27, 45]. As a first step in characterizing the transfer of fixed carbon in this relationship, we

205 compared the growth of *M. japonicum* when incubated alone or together with *C. reinhardtii* in
206 minimal medium with either no exogenous carbon source or with 150 µg/ml sucrose. While *M.*
207 *japonicum* grew considerably with sucrose and only marginally without it, we saw that coculture
208 with *C. reinhardtii* did not significantly increase the maximum bacterial density in either condition
209 (Fig. 1C, $p > 0.05$). Although the maximum density of *M. japonicum* in coculture without sucrose
210 (~$3x10^7$–$5x10^8$ CFU/ml) was similar to what has been observed previously [27], we found that the
211 bacterium was able to achieve a comparable density without the alga.

212 As the growth of *M. japonicum* was not significantly stimulated by *C. reinhardtii*, it seemed
213 that the alga did not supply adequate substrates for the bacterium's heterotrophic metabolism under
214 these conditions. This could be because *C. reinhardtii* released fixed carbon compounds in
215 insufficient quantities, or because *M. japonicum* is unable to metabolize the specific compounds
216 generated by *C. reinhardtii*. To address these possibilities, we monitored coculture growth and
217 organic carbon exchange under different light regimes, as diel light greatly alters *C. reinhardtii's*
218 metabolism [10]. During the day, the alga fixes carbon to build biomass and stores photosynthate
219 as starch. After sufficient growth during the light phase, cells initiate DNA synthesis and mitosis
220 in the dark, followed by a G0 phase during which starch reserves are degraded by glycolysis
221 followed by fermentation. We hypothesized that the alga's nighttime metabolism could stimulate
222 additional growth of *M. japonicum*.

223 To resolve diel patterns in growth and the reduced carbon content of the spent medium, we
224 used the readily synchronized *C. reinhardtii* strain CC-5390 and compared cocultures and
225 monocultures under continuous and diel light over several days with high temporal resolution.
226 Since *C. reinhardtii*'s doubling time is slower under diel light (cells only divide once per day), the
227 experiment was designed to achieve the same final amount of algal biomass under the two light

228 regimes. *C. reinhardtii* growth was unaffected by the bacterium, and algal cell density reached
229 roughly $4x10^6$ cells/ml under all conditions (Fig. 2A, 2C). On the other hand, we found that *M.*
230 *japonicum* density increased significantly in the presence of CC-5390 under both light regimes
231 (Fig. 2B, 2D). We could not discern a clear temporal pattern in bacterial proliferation over the diel
232 cycles, and contrary to our hypothesis, we found that continuous light supported 3-fold more
233 bacterial cells than did diel light (Fig. 2E). Spent medium from continuous light-grown *C.*
234 *reinhardtii* had significantly more nonpurgeable organic carbon (NPOC) than spent medium from
235 diel light-grown *C. reinhardtii* of the same culture density, suggesting that more dissolved organic
236 carbon was available to the bacterium under continuous light (Fig. 2F). However, the presence of
237 *M. japonicum* did not significantly reduce the concentration of NPOC in the spent medium. This
238 could mean that either *M. japonicum* did not take up significant amounts of organic carbon from
239 the medium or that it could not fully oxidize it to CO_2, and instead released reduced carbon waste
240 products back into the extracellular milieu.

241 **Stable isotope probing reveals mismatch between bacterial biomass synthesis and division in**
242 **coculture**

243 To determine the amount of carbon fixed by *C. reinhardtii* that is taken up by *M.*
244 *japonicum*, we conducted stable isotope probing experiments using $^{13}CO_2$. Cocultures of CC-5390
245 and *M. japonicum* grown under continuous and diel light as in Fig. 2 were bubbled with air
246 containing $^{13}CO_2$, and $^{15}NH_4Cl$ was added to the medium as an independent tracer of biomass
247 synthesis, complementing measurements of cell density. Then, we assayed label uptake by single
248 cells using nanoSIMS.

249 We found substantial ^{13}C enrichment of the algal cells at a steady concentration throughout
250 the timepoints examined (Fig. 3A, SI Fig. 2, SI Fig. 3). In addition, we observed ^{13}C enrichment

251 of bacterial cells, which increased with time in cocultures under both light regimes (Fig. 3A, SI
252 Fig. 2, SI Fig. 3). Killed controls and a monoculture of *M. japonicum* grown with sucrose
253 demonstrated that this enrichment was not a result of nonspecific background or direct CO_2
254 incorporation during heterotrophic growth (i.e. anapleurotic carboxylation reactions) (SI Fig. 3).
255 Thus, a meaningful amount of carbon derived from algal photoautotrophy was in fact incorporated
256 into *M. japonicum* biomass in these cocultures. We compared the extent of carbon transfer under
257 continuous and diel light by calculating the fraction of bacterial biomass derived from algal carbon
258 (C_{net}), using the average algal biomass ^{13}C content over the course of the experiment as a rough
259 measure of the source carbon isotopic composition. We found that significantly more algal ^{13}C
260 was transferred to bacterial cells under continuous light over 48 h (0.17 median C_{net} in continuous
261 light, 0.09 median C_{net} in diel light) (Fig. 3B), consistent with our observation that spent medium
262 NPOC and *M. japonicum* cell density were greater in cocultures exposed to continuous light than
263 to diel light (Fig. 2, SI Fig. 4).

264 Both the ^{13}C and ^{15}N enrichment in *M. japonicum* cells were lower than we had expected
265 from the increase in bacterial CFUs observed in the experiment (>3-fold increase in CFUs during
266 the first 24 h of coculture under continuous light), suggesting a mismatch between the change in
267 cell density and the bacterial biomass synthesized (Fig. 3C, SI Fig. 4). We quantified the magnitude
268 of this mismatch using the ^{15}N label, for which the source isotopic composition was better
269 constrained, as opposed to that of the ^{13}C label which was delivered in the gas phase in an open
270 system. Using the source ^{15}N composition and the measured isotopic composition of bacterial
271 ROIs at each timepoint, we calculated the fraction of newly synthesized biomass generated from
272 the source substrate over the course of the experiment (N_{net}) [44]. We compared this to the expected
273 N_{net} that would be observed if each doubling in CFUs in the culture occurred upon a doubling in

274 bacterial biomass (0.99 N_{net} for cells grown on sucrose after 8–13 doublings, 0.63–0.97 N_{net} for
275 cells co-cultivated with *C. reinhardtii* after 1–5 doublings) (SI Fig. 4). Indeed, the measured N_{net}
276 of *M. japonicum* cells in the cocultures was much lower than the expected values at all measured
277 timepoints (0.18–0.34 N_{net}), whereas the measured values matched the expected values during
278 logarithmic-phase growth on sucrose (Fig. 4A). This suggested that in coculture with *C.*
279 *reinhardtii*, *M. japonicum* cells had ceased biomass synthesis by 24 h and yet continued to divide,
280 a hallmark of bacterial starvation known as reductive division [46, 47].

281 If this deviation of the observed N_{net} from the expected N_{net} reflected reductive division of
282 *M. japonicum*, we predicted that bacterial cells in the coculture would be smaller than cells in the
283 logarithmic phase of growth on sucrose, which are typically 2 µm in length. As predicted, *M.*
284 *japonicum* exhibited a mean cell length of 1.4–1.5 µm after 24 h in the cocultures, relative to the
285 mean cell length of 2.3 µm after 24 h of growth on sucrose (Fig. 4B, 4C). When sucrose was
286 depleted from the medium over the subsequent day in the monoculture, mean cell length decreased
287 to a similar extent, demonstrating that reductive division occurs upon carbon limitation in *M.*
288 *japonicum*.

289 Taken together, these data show that photosynthetically fixed carbon was indeed
290 transferred from *C. reinhardtii* to *M. japonicum* under both continuous and diel light, and that
291 while this amount was not sufficient for balanced logarithmic-phase growth of the bacterium, it
292 allowed for a small amount of bacterial proliferation.

293 **Reductively dividing bacteria still deliver sufficient vitamin B_{12} to support growth of the B_{12}-**
294 **requiring *mete1* strain**

295 As reductive division had not previously been reported in the *C. reinhardtii-M. japonicum*
296 interaction, we wondered whether the phenomenon also occurs during coculture with the B_{12}-

297 requiring *mete1* strain of *C. reinhardtii*, and if so, whether the bacterium still synthesizes adequate
298 B_{12} to support the mutant's growth. We compared the change in bacterial cell size after growth on
299 150 µg/ml sucrose to changes during coculture with either wild-type *C. reinhardtii* or *mete1*. In all
300 conditions, we observed a 50–60% reduction in *M. japonicum* cell length over 54 h of cultivation
301 (Fig. 5A, 5B). This suggested that bacterial carbon limitation occurs to a similar extent during
302 coculture with the *mete1* strain as with the wild type. In addition, there was no significant
303 difference in *M. japonicum* density between the two cocultures (Fig. 5C).

304 To test whether reductively dividing *M. japonicum* still delivers vitamin B_{12} to *C.*
305 *reinhardtii*, we compared the growth of the *C. reinhardtii mete1* strain in coculture and
306 monoculture without exogenous B_{12}. Despite reductive division, *M. japonicum* supported
307 significant growth of the B_{12}-requiring *mete1* strain (Fig. 5D), demonstrating that bacterial B_{12}
308 synthesis and sharing still occur even under starvation.

309 While there was no difference in *M. japonicum* density after coculture with either the *C.*
310 *reinhardtii* wild type or *mete1*, there were many more *C. reinhardtii* cells present in the wild-type
311 coculture than the mutant coculture, which was B_{12}-limited (Fig. 5D). This demonstrated that
312 greater algal density does not translate into greater *M. japonicum* growth, as noted previously [27].
313 We observed this phenomenon in cocultures inoculated at several starting relative abundances (SI
314 Fig. 5). This suggests that carbon transfer from the alga to the bacterium could be indirect.

315 ***C. reinhardtii* lysis can explain observed *M. japonicum* proliferation in coculture**

316 To distinguish the source of the fixed carbon that supports *M. japonicum* proliferation in
317 coculture, we compared *M. japonicum* growth in coculture with live *C. reinhardtii* to growth in *C.*
318 *reinhardtii* spent medium and in the soluble fraction of *C. reinhardtii* cell lysate. Spent medium
319 supported the same number of *M. japonicum* cells as did coculture, demonstrating that the

320 observed increase does not require a direct interaction with the alga (Fig. 6A). Cell lysate from *C.*
321 *reinhardtii* supported almost an order of magnitude more *M. japonicum* proliferation. Therefore,
322 we hypothesized that the fixed carbon transferred in our cocultures could be sourced from a few
323 lysed *C. reinhardtii* cells rather than from photosynthate exuded by live algal cells.

324 Having determined the increase in viable *M. japonicum* cells supported by lysate from a
325 known density of *C. reinhardtii* cells (1.7×10^8 CFU/ml on average after 48 h in lysate from 1.6×10^6
326 *C. reinhardtii* cells/ml culture), we estimated the theoretical increase in *M. japonicum* CFUs
327 supported by a single lysed *C. reinhardtii* cell to be 101.5±42.8 CFU in 48 h. From that, we
328 estimated how many *C. reinhardtii* cells would have to lyse in the coculture to enable the *M.*
329 *japonicum* proliferation observed: roughly 1.1×10^5 *C. reinhardtii* cells/ml, which corresponds to
330 1.8% of the *C. reinhardtii* populations in those cocultures. To test the actual degree of algal lysis
331 in our cultures, we measured algal cellular integrity using the CellTox Green Cytotoxicity Assay.
332 This assay uses a membrane-impermeable DNA dye, resulting in fluorescence from cells whose
333 plasma membrane has been compromised or from extracellular DNA [48]. We compared live
334 culture fluorescence to killed control samples and found that 1–3% of the wild-type *C. reinhardtii*
335 population had compromised cellular integrity (Fig. 6B). Thus, the fraction of dead or dying *C.*
336 *reinhardtii* cells measured by this assay is comparable to that needed to explain the observed *M.*
337 *japonicum* proliferation. These data are consistent with the interpretation that *M. japonicum*
338 growth in coculture is enabled by substrates that are released through *C. reinhardtii* cell lysis,
339 rather than by substrates exuded by live *C. reinhardtii* cells.

340 **DISCUSSION**

341 Most studies of symbioses between *C. reinhardtii* and heterotrophic bacteria to date have
342 focused on impacts on the alga, leaving open the question of how this model phototroph might

343 influence bacterial growth and physiology. Here, we have investigated *C. reinhardtii's* role as a
344 primary producer in the established coculture system with *M. japonicum*. Under continuous light,
345 we found that the alga increased the number of viable bacterial cells, albeit marginally so. We
346 tested whether nighttime metabolism might increase the alga's propensity for carbon sharing but
347 found that diel illumination actually decreased the productivity of the partnership. Using single-
348 cell analysis of ^{13}C enrichment by nanoSIMS, we quantitatively demonstrated transfer of carbon
349 fixed by the model alga to the bacterium. Roughly 17% of the carbon in *M. japonicum* cells was
350 derived from *C. reinhardtii* over 36 h under continuous light, whereas only ~9% of the *M.*
351 *japonicum* carbon came from *C. reinhardtii* over the same amount of time under diel light. Bulk
352 measurements showed that algal cultures of similar densities had more organic carbon in their
353 spent medium after continuous illumination than after diel illumination. Together, these results
354 suggest that the increased metabolic rate realized under continuous light may be more beneficial
355 for *M. japonicum* (and potentially other bacteria) than algal nighttime catabolism of starch.

356 With *C. reinhardtii* as the sole source of fixed carbon, *M. japonicum* exhibited signs of
357 starvation, even under continuous light, highlighting the meagerness of the microbial trophic
358 relationship. The quantitative stable isotope probing experiments revealed that during coculture
359 with *C. reinhardtii*, *M. japonicum* synthesized significantly less biomass than expected, given the
360 increase in viable bacterial cells. By direct measurement, we showed that *M. japonicum* undergoes
361 reductive division in coculture, dividing into small daughter cells within 24 h of carbon limitation.
362 Studies on freshwater and marine bacteria have similarly documented up to 90% reduction in cell
363 volume during carbon limitation [49–52]. Reductive division is a common strategy for surviving
364 starvation and has been studied in many Gram-negative bacteria including *Escherichia*, *Klebsiella*,
365 *Vibrio*, *Pseudomonas*, and *Rhizobium* species [46, 47]. By increasing cell number and reducing

366 cell volume, these bacteria increase the probability that a member of the population will encounter
367 sufficient nutrients again and increase their surface area-to-volume ratio to improve nutrient
368 uptake. Reductively dividing cells also exhibit changes in macromolecule synthesis and stress
369 resistance. Importantly though, we found that despite its apparent starvation, *M. japonicum*
370 provided enough vitamin B_{12} to support a B_{12}-dependent *C. reinhardtii* mutant. Vitamin supply
371 enables growth of auxotrophs, influences gene expression and metabolism, and can even give rise
372 to vitamin dependency in algae [25, 53]. Thus, our results suggest that even under austere
373 conditions with meager supply of growth substrates, bacteria can still influence algal physiology
374 and evolution.

375 We also found that a direct interaction with *C. reinhardtii* was not required to achieve the
376 *M. japonicum* proliferation observed in coculture: growth in algal spent medium yielded the same
377 maximum density of viable *M. japonicum* cells as did coculture. Furthermore, mechanically lysed
378 *C. reinhardtii* cells yielded considerably higher *M. japonicum* densities. This observation led us to
379 hypothesize that perhaps this bacterium does not metabolize the exudates of live *C. reinhardtii*
380 cells at all. Instead, perhaps the small amount of bacterial growth observed in coculture and in
381 spent medium is due to the death of a small fraction of algal cells. It has long been appreciated that
382 even during rapid exponential growth, microbial cultures experience a small death rate [54].
383 Furthermore, cell lysis is an important mechanism of nutrient transfer in natural environments, and
384 microbial necromass is a major component of the soil organic carbon pool [55, 56]. For the
385 experimental conditions examined here, we showed that ~2% of the *C. reinhardtii* population in
386 our cultures are present as necromass. Based on the *M. japonicum* growth yields achieved in
387 mechanically lysed *C. reinhardtii* cells, we calculated that this is almost exactly the amount of
388 algal necromass required to explain the degree of *M. japonicum* proliferation that occurred in

389 coculture. Therefore, we propose that lysis is the primary mechanism of trophic transfer in this
390 coculture system, rather than exudation or direct exchange.

391 Given that very little growth of *M. japonicum* was observed from an interaction with *C.*
392 *reinhardtii* – even under conditions optimized for algal productivity – our results may suggest that
393 this model alga exhibits a low carrying capacity for heterotrophic bacteria in the environment.
394 Similar bacterial densities have been reported for other *C. reinhardtii* cocultures in minimal media,
395 including those with *Methylobacterium aquaticum* [29, 57]. On the other hand, it is possible that
396 other bacteria, such as those that may have co-evolved with *C. reinhardtii* in its native
397 environment, may possess greater capacity to metabolize compounds that *C. reinhardtii* releases
398 during growth or may achieve greater access to growth substrates through chemotaxis, interspecies
399 signaling and direct exchange, or algicidal activity [3, 58–61]. In addition, the mode of cell lysis
400 (i.e. mechanical vs. viral) can greatly impact the nutrients released [62]. Yet, the system studied
401 here has revealed important aspects of algal-bacterial interactions, and our quantitative approach
402 can serve as a roadmap for the future work necessary to understand *C. reinhardtii*'s full potential
403 as a primary producer in the microbial world.

404 **ACKNOWLEDGEMENTS**

405 This work was supported by The Gordon and Betty Moore Foundation Symbiosis in Aquatic
406 Systems Initiative Investigator Award GBML9203, and the Lawrence Livermore National
407 Laboratory μBiospheres Scientific Focus Area award SCW1039 from the DOE OBER Genomic
408 Sciences Program. S.D. acknowledges support from NIH T32 Genetic Dissection of Cells and
409 Organisms training grant 1T32GM132022-01. We thank Dr. Alison G. Smith and her group at the
410 University of Cambridge for providing strains and for their generous discussions with us. We thank
411 Dr. Michiko E. Taga at UC Berkeley for her guidance on the work. We thank Dr. Denise Schichnes

412 and the UC Berkeley Biological Imaging Facility for fluorescence microscopy support. We also
413 thank Christina Ramon at Lawrence Livermore National Laboratory and Charles Perrino at UC
414 Berkeley for analytical support.

415 **COMPETING INTERESTS**

416 The authors declare no competing financial interests.

417 **DATA AVAILABILITY**

418 All data underlying this article are available in Supplementary Data File S1.

419 **REFERENCES**

420 1. Field CB, Behrenfeld MJ, Randerson JT, Falkowski P. Primary Production of the
421 Biosphere: Integrating Terrestrial and Oceanic Components. *Science* 1998; **281**: 237–240.
422 2. Azam F, Fenchel T, Field J, Gray J, Meyer-Reil L, Thingstad F. The Ecological Role of
423 Water-Column Microbes in the Sea. *Mar Ecol Prog Ser* 1983; **10**: 257–263.
424 3. Seymour JR, Amin SA, Raina J-B, Stocker R. Zooming in on the phycosphere: the
425 ecological interface for phytoplankton–bacteria relationships. *Nat Microbiol* 2017; **2**:
426 17065.
427 4. Pomeroy LR. The Ocean's Food Web, A Changing Paradigm. *Bioscience* 1974; **24**: 499–
428 504.
429 5. Azam F, Malfatti F. Microbial structuring of marine ecosystems. *Nat Rev Microbiol* 2007;
430 **5**: 782–791.
431 6. Croft MT, Lawrence AD, Raux-Deery E, Warren MJ, Smith AG. Algae acquire vitamin
432 B_{12} through a symbiotic relationship with bacteria. *Nature* 2005; **438**: 90–93.

433 7. Amin SA, Green DH, Hart MC, Küpper FC, Sunda WG, Carrano CJ. Photolysis of iron–
434 siderophore chelates promotes bacterial–algal mutualism. *Proc Natl Acad Sci* 2009; **106**:
435 17071–17076.
436 8. Hom EFY, Aiyar P, Schaeme D, Mittag M, Sasso S. A Chemical Perspective on
437 Microalgal-Microbial Interactions. *Trends Plant Sci* 2015; **20**: 689–693.
438 9. Salomé PA, Merchant SS. A Series of Fortunate Events: Introducing Chlamydomonas as a
439 Reference Organism. *Plant Cell* 2019; **31**: 1682–1707.
440 10. Strenkert D, Schmollinger S, Gallaher SD, Salomé PA, Purvine SO, Nicora CD, *et al.*
441 Multiomics resolution of molecular events during a day in the life of Chlamydomonas.
442 *Proc Natl Acad Sci* 2019; **116**: 2374–2383.
443 11. Zones JM, Blaby IK, Merchant SS, Umen JG. High-resolution profiling of a synchronized
444 diurnal transcriptome from *Chlamydomonas reinhardtii* reveals continuous cell and
445 metabolic differentiation. *Plant Cell* 2015; **27**: 2743–2769.
446 12. Durán P, Flores-Uribe J, Wippel K, Zhang P, Guan R, Melkonian B, *et al.* Shared features
447 and reciprocal complementation of the Chlamydomonas and Arabidopsis microbiota. *Nat*
448 *Commun* 2022; **13**: 406.
449 13. Kim B-H, Ramanan R, Cho D-H, Oh H-M, Kim H-S. Role of Rhizobium, a plant growth
450 promoting bacterium, in enhancing algal biomass through mutualistic interaction. *Biomass*
451 *Bioenergy* 2014; **69**: 95–105.
452 14. Lőrincz Z, Preininger É, Kósa A, Pónyi T, Nyitrai P, Sarkadi L, *et al.* Artificial tripartite
453 symbiosis involving a green alga (Chlamydomonas), a bacterium (Azotobacter) and a
454 fungus (Alternaria): Morphological and physiological characterization. *Folia Microbiol*
455 *(Praha)* 2010; **55**: 393–400.

456 15. Xie B, Bishop S, Stessman D, Wright D, Spalding MH, Halverson LJ. *Chlamydomonas*
457 *reinhardtii* thermal tolerance enhancement mediated by a mutualistic interaction with
458 vitamin B_{12}-producing bacteria. *ISME J* 2013; **7**: 1544–1555.
459 16. Amin SA, Parker MS, Armbrust EV. Interactions between Diatoms and Bacteria.
460 *Microbiol Mol Biol Rev* 2012; **76**: 667–684.
461 17. Gobler C, Norman C, Panzeca C, Taylor G, Sañudo-Wilhelmy S. Effect of B-vitamins
462 (B_1, B_{12}) and inorganic nutrients on algal bloom dynamics in a coastal ecosystem. *Aquatic*
463 *Microbial Ecol* 2007; **49**: 181–194.
464 18. Sañudo-Wilhelmy SA, Gobler CJ, Okbamichael M, Taylor GT. Regulation of
465 phytoplankton dynamics by vitamin B_{12}. *Geophys Res Lett* 2006; **33**: L04604.
466 19. Helliwell KE. The roles of B vitamins in phytoplankton nutrition: new perspectives and
467 prospects. *New Phytol* 2017; **216**: 62–68.
468 20. Keshtacher-Liebso E, Hadar Y, Chen Y. Oligotrophic Bacteria Enhance Algal Growth
469 under Iron-Deficient Conditions. *Appl Environ Microbiol* 1995; **61**: 2439–41.
470 21. Fakhimi N, Gonzalez-Ballester D, Fernández E, Galván A, Dubini A. Algae-Bacteria
471 Consortia as a Strategy to Enhance H_2 Production. *Cells* 2020; **9**: 1353.
472 22. Krespach MKC, Stroe MC, Flak M, Komor AJ, Nietzsche S, Sasso S, *et al.* Bacterial
473 marginolactones trigger formation of algal gloeocapsoids, protective aggregates on the
474 verge of multicellularity. *Proc Natl Acad Sci* 2021; **118**.
475 23. Windler M, Stuart R, Deutzmann JS, Mayali X, Navid A, D'haeseleer P, *et al.* Bacterial
476 exometabolites influence *Chlamydomonas* cell cycle and double algal productivity. *FEMS*
477 *Microbiol Ecol* 2022; **98**.

478 24. Kazamia E, Czesnick H, Nguyen TT Van, Croft MT, Sherwood E, Sasso S, *et al.*
479 Mutualistic interactions between vitamin B_{12}-dependent algae and heterotrophic bacteria
480 exhibit regulation. *Environ Microbiol* 2012; **14**: 1466–1476.
481 25. Helliwell KE, Collins S, Kazamia E, Purton S, Wheeler GL, Smith AG. Fundamental shift
482 in vitamin B_{12} eco-physiology of a model alga demonstrated by experimental evolution.
483 *ISME J* 2015; **9**: 1446–1455.
484 26. Bunbury F, Helliwell KE, Mehrshahi P, Davey MP, Salmon DL, Holzer A, *et al.*
485 Responses of a Newly Evolved Auxotroph of Chlamydomonas to B_{12} Deprivation. *Plant*
486 *Physiol* 2020; **183**: 167–178.
487 27. Bunbury F, Deery E, Sayer AP, Bhardwaj V, Harrison EL, Warren MJ, *et al.* Exploring
488 the onset of B_{12}-based mutualisms using a recently evolved Chlamydomonas auxotroph
489 and B_{12}-producing bacteria. *Environ Microbiol* 2022; **24**: 3134–3147.
490 28. Helliwell KE, Scaife MA, Sasso S, Araujo APU, Purton S, Smith AG. Unraveling
491 Vitamin B_{12}-Responsive Gene Regulation in Algae. *Plant Physiol* 2014; **165**: 388–397.
492 29. Calatrava V, Hom EFY, Llamas Á, Fernández E, Galván A. OK, thanks! A new
493 mutualism between Chlamydomonas and methylobacteria facilitates growth on amino
494 acids and peptides. *FEMS Microbiol Lett* 2018; **365**.
495 30. Dubini A, Mus F, Seibert M, Grossman AR, Posewitz MC. Flexibility in Anaerobic
496 Metabolism as Revealed in a Mutant of *Chlamydomonas reinhardtii* Lacking
497 Hydrogenase Activity. *J Biol Chem* 2009; **284**: 7201–7213.
498 31. Gfeller RP, Gibbs M. Fermentative Metabolism of *Chlamydomonas reinhardtii*. *Plant*
499 *Physiol* 1984; **75**: 212–218.

500 32. Mus F, Dubini A, Seibert M, Posewitz MC, Grossman AR. Anaerobic Acclimation in
501 *Chlamydomonas reinhardtii*. *J Biol Chem* 2007; **282**: 25475–25486.
502 33. Yang W, Catalanotti C, Wittkopp TM, Posewitz MC, Grossman AR. Algae after dark:
503 mechanisms to cope with anoxic/hypoxic conditions. *Plant J* 2015; **82**: 481–503.
504 34. Ghirardi ML, Subramanian V, Wecker MSA, Smolinski S, Antonio RV, Xiong W, *et al.*
505 Survey of the anaerobic metabolism of various laboratory wild-type *Chlamydomonas*
506 *reinhardtii* strains. *Algal Res* 2018; **35**: 355–361.
507 35. Nishio K, Hashimoto K, Watanabe K. Light/electricity conversion by defined cocultures
508 of Chlamydomonas and Geobacter. *J Biosci Bioeng* 2013; **115**: 412–417.
509 36. Lodwig E, Poole P. Metabolism of *Rhizobium* Bacteroids. *CRC Crit Rev Plant Sci* 2003;
510 **22**: 37–78.
511 37. Ronson CW, Lyttleton P, Robertson JG. C_4-dicarboxylate transport mutants of *Rhizobium*
512 *trifolii* form ineffective nodules on *Trifolium repens*. *Proc Natl Acad Sci* 1981; **78**: 4284–
513 4288.
514 38. Finan TM, Oresnik I, Bottacin A. Mutants of *Rhizobium meliloti* defective in succinate
515 metabolism. *J Bacteriol* 1988; **170**: 3396–3403.
516 39. Geddes BA, Oresnik IJ. Physiology, genetics, and biochemistry of carbon metabolism in
517 the alpha-proteobacterium *Sinorhizobium meliloti*. *Can J Microbiol* 2014; **60**: 491–507.
518 40. Zhalnina K, Louie KB, Hao Z, Mansoori N, da Rocha UN, Shi S, *et al.* Dynamic root
519 exudate chemistry and microbial substrate preferences drive patterns in rhizosphere
520 microbial community assembly. *Nat Microbiol* 2018; **3**: 470–480.
521 41. Sueoka N. MITOTIC REPLICATION OF DEOXYRIBONUCLEIC ACID IN
522 CHLAMYDOMONAS REINHARDI. *Proc Natl Acad Sci* 1960; **46**: 83–91.

523 42. Kropat J, Hong-Hermesdorf A, Casero D, Ent P, Castruita M, Pellegrini M, *et al.* A
524 revised mineral nutrient supplement increases biomass and growth rate in
525 *Chlamydomonas reinhardtii*. *Plant J* 2011; **66**: 770–780.
526 43. Lingappa UF, Dupuis S, Mayali X, Merchant SS. Isotopically labelled inorganic carbon
527 delivered to algal cultures via bubbler bottle. *protocols.io* 2023.
528 44. Dekas AE, Parada AE, Mayali X, Fuhrman JA, Wollard J, Weber PK, *et al.*
529 Characterizing Chemoautotrophy and Heterotrophy in Marine Archaea and Bacteria With
530 Single-Cell Multi-isotope NanoSIP. *Front Microbiol* 2019; **10**.
531 45. Laeverenz Schlogelhofer H, Peaudecerf FJ, Bunbury F, Whitehouse MJ, Foster RA, Smith
532 AG, *et al.* Combining SIMS and mechanistic modelling to reveal nutrient kinetics in an
533 algal-bacterial mutualism. *PLoS One* 2021; **16**: e0251643.
534 46. Thorne SH, Williams HD. Adaptation to nutrient starvation in *Rhizobium leguminosarum*
535 *bv. phaseoli*: analysis of survival, stress resistance, and changes in macromolecular
536 synthesis during entry to and exit from stationary phase. *J Bacteriol* 1997; **179**: 6894–
537 6901.
538 47. Shimaya T, Okura R, Wakamoto Y, Takeuchi KA. Scale invariance of cell size
539 fluctuations in starving bacteria. *Commun Phys* 2021; **4**: 238.
540 48. Haire TC, Bell C, Cutshaw K, Swiger B, Winkelmann K, Palmer AG. Robust Microplate-
541 Based Methods for Culturing and in Vivo Phenotypic Screening of *Chlamydomonas*
542 *reinhardtii*. *Front Plant Sci* 2018; **9**.
543 49. Vrede K, Heldal M, Norland S, Bratbak G. Elemental composition (C, N, P) and cell
544 volume of exponentially growing and nutrient-limited bacterioplankton. *Appl Environ*
545 *Microbiol* 2002; **68**: 2965–71.

546 50. Troussellier M, Bouvy M, Courties C, Dupuy C. Variation of carbon content among
547 bacterial species under starvation condition. *Aquatic Microbial Ecol* 1997; **13**: 113–119.
548 51. Holmquist L, Kjelleberg S. Changes in viability, respiratory activity and morphology of
549 the marine Vibrio sp. strain S14 during starvation of individual nutrients and subsequent
550 recovery. *FEMS Microbiol Ecol* 1993; **12**: 215–223.
551 52. Mårdén P, Tunlid A, Malmcrona-Friberg K, Odham G, Kjelleberg S. Physiological and
552 morphological changes during short term starvation of marine bacterial isolates. *Arch*
553 *Microbiol* 1985; **142**: 326–332.
554 53. Sokolovskaya OM, Shelton AN, Taga ME. Sharing vitamins: Cobamides unveil microbial
555 interactions. *Science* 2020; **369**.
556 54. Kelly CD, Rahn O. The Growth Rate of Individual Bacterial Cells. *J Bacteriol* 1932; **23**:
557 147–153.
558 55. Gude S, Pherribo GJ, Taga ME. Emergence of Metabolite Provisioning as a By-Product of
559 Evolved Biological Functions. *mSystems* 2020; **5**.
560 56. Sokol NW, Slessarev E, Marschmann GL, Nicolas A, Blazewicz SJ, Brodie EL, *et al.* Life
561 and death in the soil microbiome: how ecological processes influence biogeochemistry.
562 *Nat Rev Microbiol* 2022; **20**: 415–430.
563 57. Ban S, Lin W, Wu F, Luo J. Algal-bacterial cooperation improves algal photolysis-
564 mediated hydrogen production. *Bioresour Technol* 2018; **251**: 350–357.
565 58. Samo TJ, Kimbrel JA, Nilson DJ, Pett-Ridge J, Weber PK, Mayali X. Attachment
566 between heterotrophic bacteria and microalgae influences symbiotic microscale
567 interactions. *Environ Microbiol* 2018; **20**: 4385–4400.

568 59. Jackrel SL, Yang JW, Schmidt KC, Denef VJ. Host specificity of microbiome assembly
569 and its fitness effects in phytoplankton. *ISME J* 2021; **15**: 774–788.
570 60. Aiyar P, Schaeme D, García-Altares M, Carrasco Flores D, Dathe H, Hertweck C, *et al.*
571 Antagonistic bacteria disrupt calcium homeostasis and immobilize algal cells. *Nat*
572 *Commun* 2017; **8**: 1756.
573 61. Raina J-B, Giardina M, Brumley DR, Clode PL, Pernice M, Guagliardo P, *et al.*
574 Chemotaxis increases metabolic exchanges between marine picophytoplankton and
575 heterotrophic bacteria. *Nat Microbiol* 2023; **8**: 510–521.
576 62. Pherribo GJ, Taga ME. Bacteriophage-mediated lysis supports robust growth of amino
577 acid auxotrophs. *ISME J* 2023; **17**: 1785–1788.
578
579

FIGURES

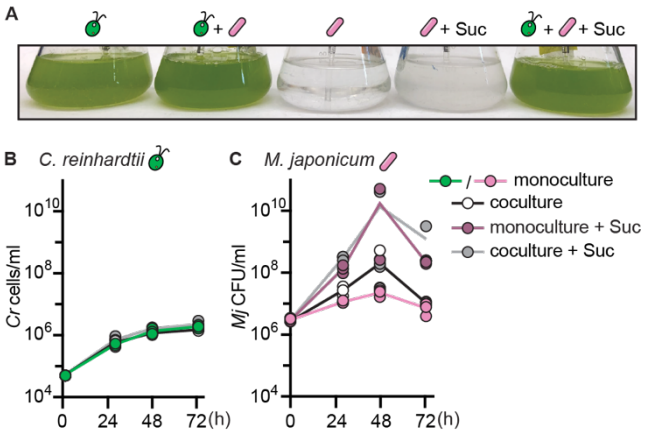

Figure 1: *C. reinhardtii* does not significantly improve growth of *M. japonicum*. Triplicate cultures (n = 3) were inoculated with or without sucrose and maintained under continuous light, bubbled with air, and shaken at 110 rpm. (A) Representative image of cultures 72 h after inoculation. (B) Wild-type *C. reinhardtii* cell density in cultures over time after inoculation. (C) *M. japonicum* cell density in cultures over time after inoculation.

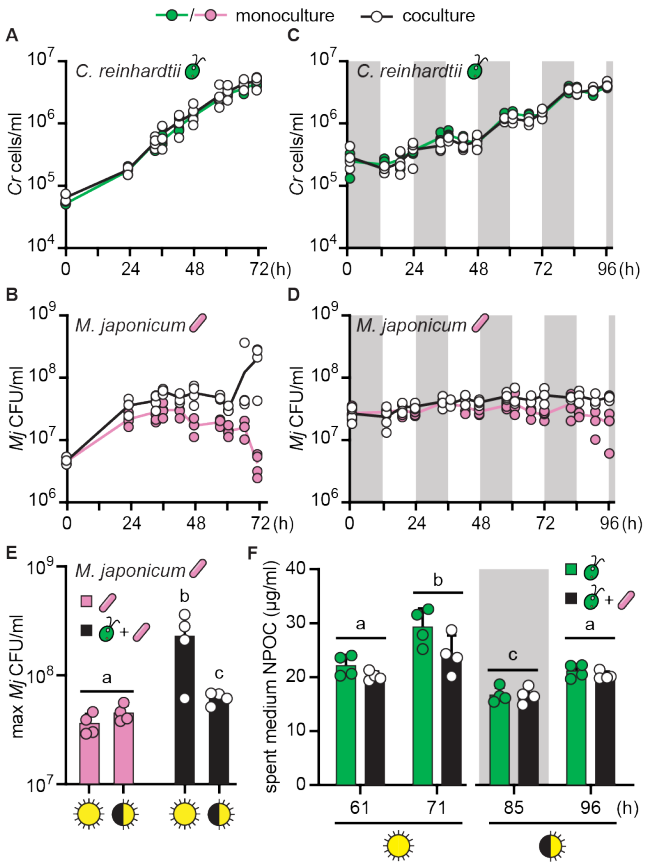

Figure 2: Coculture light regime impacts organic carbon release and *M. japonicum* growth. Quadruplicate (n = 4) monocultures (colors) and cocultures (black and white) were bubbled with air, and shaken at 125 rpm. (A, C) Growth of cell wall reduced strain CC-5390 in continuous light or diel (12-h-light/12-h-dark) light, respectively, with and without *M. japonicum*. The grey backgrounds indicate sample timepoints that occurred during the dark phase. Under diel light, CC-5390 exhibits synchronous growth, doubling roughly once per day upon nightfall. Cultures were inoculated to reach the same final algal cell density at the end of the experiment. (B, D) *M. japonicum* growth under the continuous and diel light regimes, respectively, with and without CC-5390. (E) Maximum bacterial density achieved under the various trophic conditions tested. Asterisks indicate significant differences by Student's t-test ($p < 0.05$). (F) NPOC in spent medium from CC-5390 and cocultures sampled at the indicated times from the continuous and diel light regimes in (A) and (C), respectively. Lower-case letters indicate significantly different groups by paired Student's t-test ($p < 0.05$). Error bars represent the standard deviation from the mean.

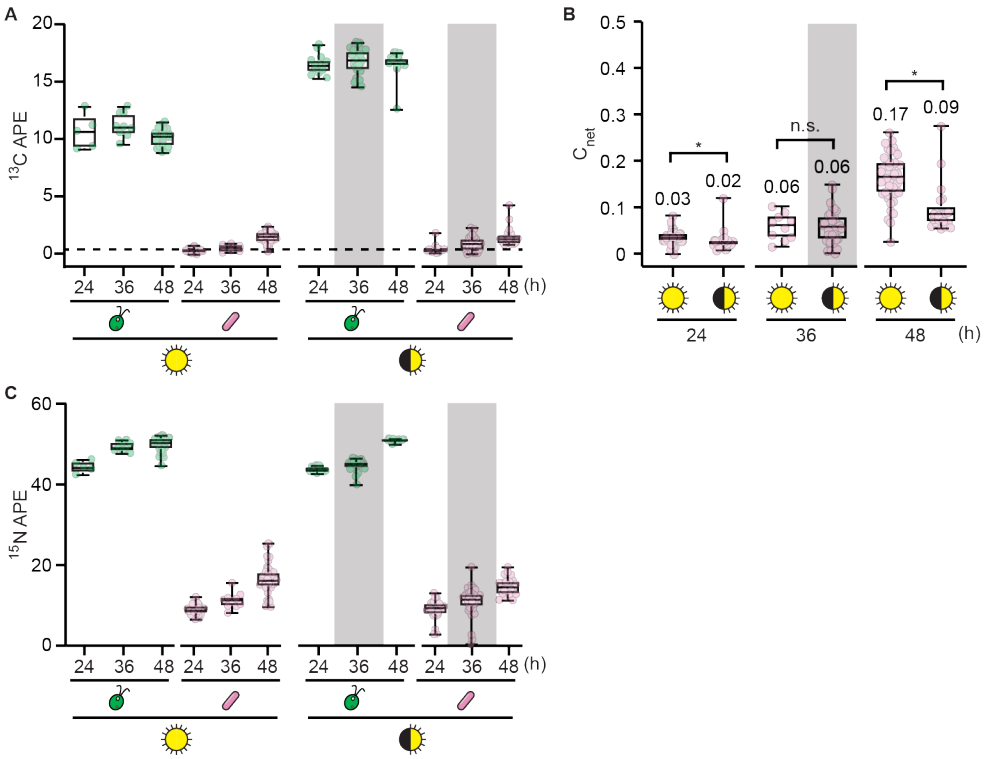

Figure 3: Stable isotope probing demonstrates carbon flux in continuous and diel light. Duplicate cocultures (n = 2) of CC-5390 and *M. japonicum* were grown as described in Fig. 2 but with 50% of their NH_4^+ provided as ^{15}N and with $^{13}CO_2$ added to the air used to bubble the cultures starting 13 h after inoculation. Isotope enrichment was measured using nanoSIMS at the indicated times after inoculation. The grey backgrounds indicate sample timepoints that occurred during the dark phase. (A) ^{13}C atom percent enrichment (APE) data of $n \geq 5$ individual cells grown under continuous light or diel light. The dashed lines represent the maximum ^{13}C APE that occurred in *M. japonicum* monoculture controls provided sucrose as a result of nonspecific background or direct CO_2 incorporation during heterotrophic growth; see SI Fig. 3 for more details. (B) C_{net} of *M. japonicum* cells ($n \geq 10$), calculated relative the algal biomass as the source. Median values are indicated, and asterisks indicate significant differences by Student's t-test ($p < 0.05$). (C) ^{15}N APE data of $n \geq 5$ individual cells grown under continuous light or diel light.

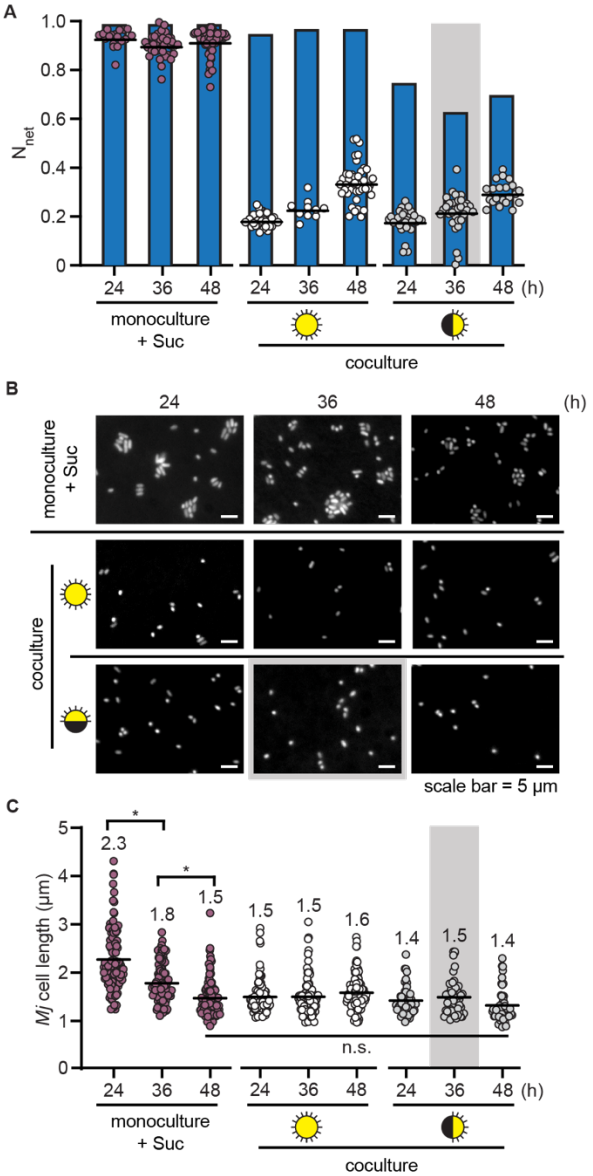

Figure 4: *M. japonicum* undergoes reductive division upon depletion of sucrose and during algal coculture. Duplicate cultures (n = 2) (monoculture with 150 µg/ml sucrose (pink) or coculture under continuous light (white) or diel light (grey)) were grown as described in Fig. 2 but with 50% of their NH_4^+ provided as ^{15}N and with $^{13}CO_2$ added to the air used to bubble the cultures starting 13 h after inoculation. Isotope enrichment was measured using nanoSIMS and cells were imaged by fluorescence microscopy at the indicated times after inoculation. The grey backgrounds indicate sample timepoints that occurred during the dark phase. (A) N_{net} *M. japonicum* cells ($n \geq 10$) (circles) relative to the calculated expected N_{net} (blue bars) if each doubling in CFU/ml (SI Fig. 4) represented a doubling in biomass; black lines represent mean values. (B) Representative fluorescence microscopy images of cells stained with DAPI. (C) Cell length of $n \geq 50$ *M. japonicum* cells per culture type measured using ImageJ. Mean cell length is indicated, and asterisks indicate significant differences by Student's t-test ($p < 0.05$).

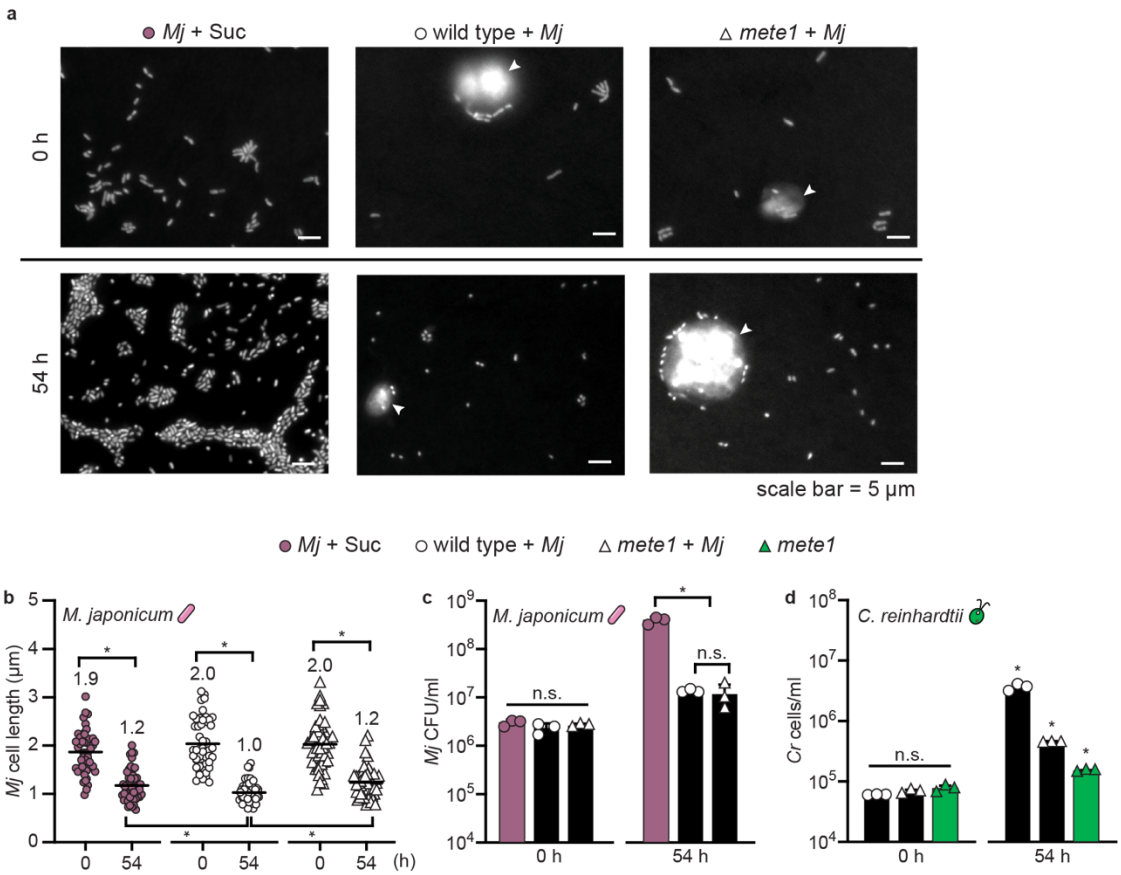

Figure 5: *M. japonicum* delivers vitamin B_{12} to *C. reinhardtii* despite reductive division. Triplicate cultures (n = 3) were maintained under continuous light and shaken at 130 rpm for 54 h after inoculation. (A) Representative fluorescence microscopy images of *M. japonicum* monoculture with 150 µg/ml sucrose, coculture of *C. reinhardtii* wild type and *M. japonicum*, and coculture of *C. reinhardtii mete1* and *M. japonicum* stained with DAPI. *C. reinhardtii* cells are indicated with white arrowheads. (B) Cell length of *M. japonicum* cells (n = 50) per culture type was measured using ImageJ. Mean cell length is indicated. (C) *M. japonicum* density in monoculture with 150 µg/ml sucrose (pink bars) or in coculture (black bars) with wild-type (circles) and *mete1 C. reinhardtii* (triangles), estimated as CFU. (D) Cell density of *C. reinhardtii* wild type (circles) or *mete1* (triangles) in coculture (black bars) and of *mete1* alone without vitamin B_{12} (green bars). Error bars represent the standard deviation from the mean, and asterisks indicate significant difference ($p < 0.05$).

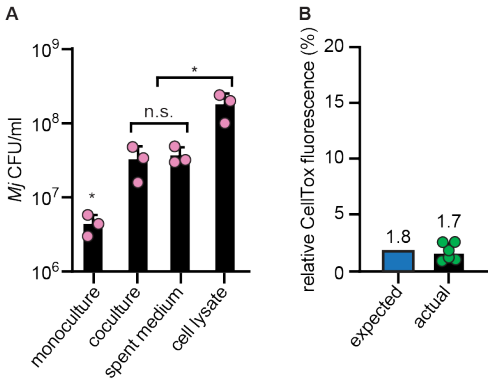

Figure 6: A small degree of algal lysis can explain the *M. japonicum* growth that occurs in coculture. Triplicate cultures (n = 3) of wild-type *C. reinhardtii* were grown under continuous light and shaken at 125 rpm for 24 h, reaching 1–4x10^6 cells/ml. These cultures were then split and used to generate parallel live algal cultures, algal spent media, and algal cell lysate, each then inoculated with *M. japonicum* in triplicate (n = 3). (A) *M. japonicum* density 45 h after inoculation in monoculture with no reduced carbon source, coculture with live *C. reinhardtii cells*, *C. reinhardtii* spent medium, or *C. reinhardtii* cell lysate. Asterisks indicate significant differences by Student's t-test ($p < 0.05$). (B) The approximate degree of *C. reinhardtii* cell lysis required to explain *M. japonicum* growth in coculture based on *M. japonicum* growth yield in *C. reinhardtii* cell lysate (blue bar), and the degree of *C. reinhardtii* cell lysis measured in the cultures used for the experiment in panel (A) by CellTox Green, reported relative to a 100% killed control. The expected value and the mean value are indicated. Error bars represent the standard deviation from the mean.